PBK model application in species and route to route extrapolation

Contents

Part I. PBK model reporting template

A. Name of model

PBK model application in interspecies and route to route extrapolation

B. Contact details

Authors: Jos G.M.Bessems

Affiliation: European Commission, Joint Research Centre, Ispra, Italy

C. Summary of model characterisation, development, validation, and regulatory applicability

The present paper presents a methodological case study that uses a margin of internal exposure (MOIE) approach to characterise the risk of caffeine exposure in a dermal product using data based on an oral bioassay (Fig. 1). Caffeine was chosen for this case study for oral-to-dermal extrapolation since it is an ingredient in cosmetics and oral animal toxicity data are present. A rat PBK model was developed for caffeine to convert the chosen oral NOAEL to the internal dose metrics AUC and C_{max} of caffeine, as well as of its most relevant metabolite paraxanthine. Secondly, we used an oral human PBK model (Gajewska et al., 2014, Gajewska et al., 2015) to predict human internal dose metrics. Data from an oral human volunteer study were used to calibrate some of the PBK model parameters. Subsequently, the calibrated human oral model was extended with a dermal compartment to accommodate a few realistic exposure scenarios involving the topical use of cosmetic products. QSARs were used to simulate human dermal penetration. Finally, the resulting internal dose metrics for the rat (oral) and the human (dermal) were compared in terms of resulting MOIE. With the present work we cover the extrapolations oral to dermal, high rat to low human as well as single to repeated.

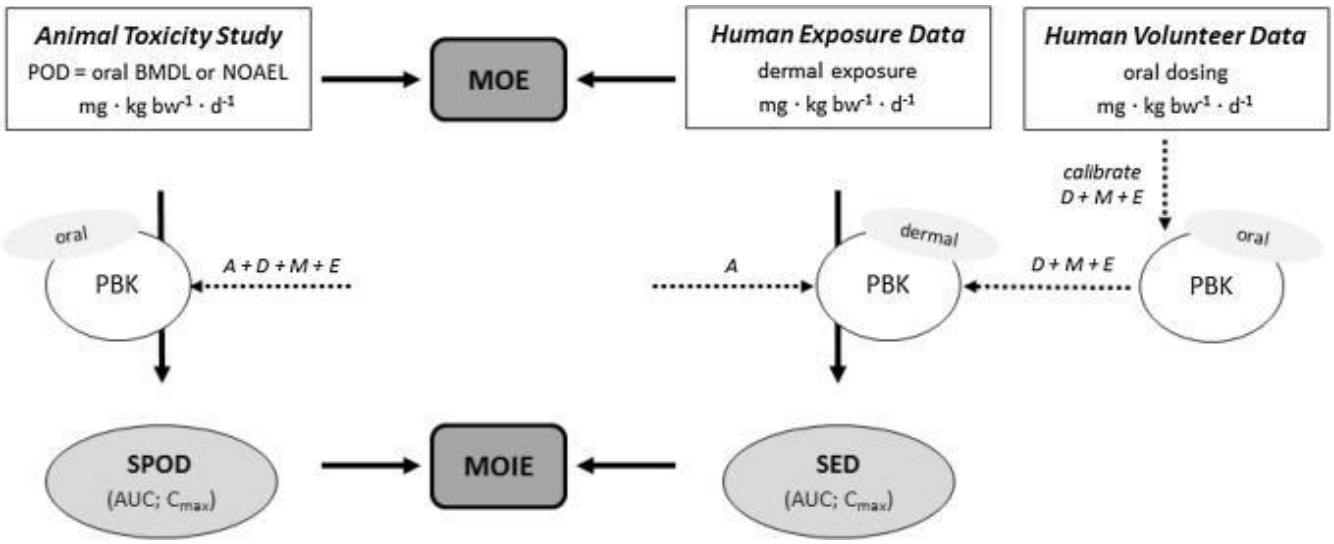

Figure 1 Conceptual depiction of the margin of internal exposure (MOIE) approach based on comparison of internal dose metrics. The individual assessment factor (AF) of 4 that should cover interspecies differences in toxicokinetics (TK) can be left out in the MOIE approach as these differences are taking into account using the PBK approach (animal PBK model and human PBK model). aPBK = animal PBK model; hPBK = human PBK model. SED = Systemic exposure dose; SPOD = Systemic Point of Departure.

D. Model characterisation (modelling workflow)

Step 1 – Scope and purpose of the model (problem formulation)

Route-to-route extrapolation is a common part of human risk assessment. Data from oral animal toxicity studies are commonly used to assess the safety of various but specific human dermal exposure scenarios. Using theoretical examples of various user scenarios, it was concluded that delineation of a generally applicable human dermal limit value is not a practicable approach, due to the wide variety of possible human exposure scenarios, including its consequences for internal exposure. Using physiologically based kinetic (PBK) modelling approaches to predict animal and human internal exposure dose metrics provides excellent opportunities to investigate the consequences of variations in human dermal exposure scenarios.

Step 2 – Model conceptualisation (model structure, mathematical representation)

A rat PBK model was developed for caffeine to convert the chosen oral NOAEL to the internal dose metrics AUC and C_{max} of caffeine, as well as of its most relevant metabolite paraxanthine. Secondly, we used an oral human PBK model (Gajewska et al., 2014, Gajewska et al., 2015) to predict human internal dose metrics. Data from an oral human volunteer study were used to calibrate some of the PBK model parameters. Subsequently, the calibrated human oral model was extended with a dermal compartment to accommodate a few realistic exposure scenarios involving the topical use of cosmetic products. QSARs were used to simulate human dermal penetration. Finally, the resulting internal dose metrics for the rat (oral) and the human (dermal) were compared in terms of resulting MOIE. With the present work we cover the extrapolations oral to dermal, high rat to low human dose metric as well as single to repeated.

QSAR modelling was used to predict dermal absorption, this information was needed for the human dermal PBK model. The various theoretical models were applied and integrated in order to develop an approach for

assessing dermal bioavailability. Parts of the human PBK model were published before (Gajewska et al., 2014, Gajewska et al., 2015). The dermal human model was based on the oral human PBK model (Gajewska et al., 2014). The oral rat model was developed for the current project by replacing in the human model the human parameters with the rat parameters (rat physiology and anatomy, see appendix). Chemical specific parameters were kept the same as in the human model which had been set after optimization to the human volunteer blood data (Gajewska et al., 2014). See Fig.2 for the overall PBK model structures. PBK model assumptions are reported under (D) Model characterisation.

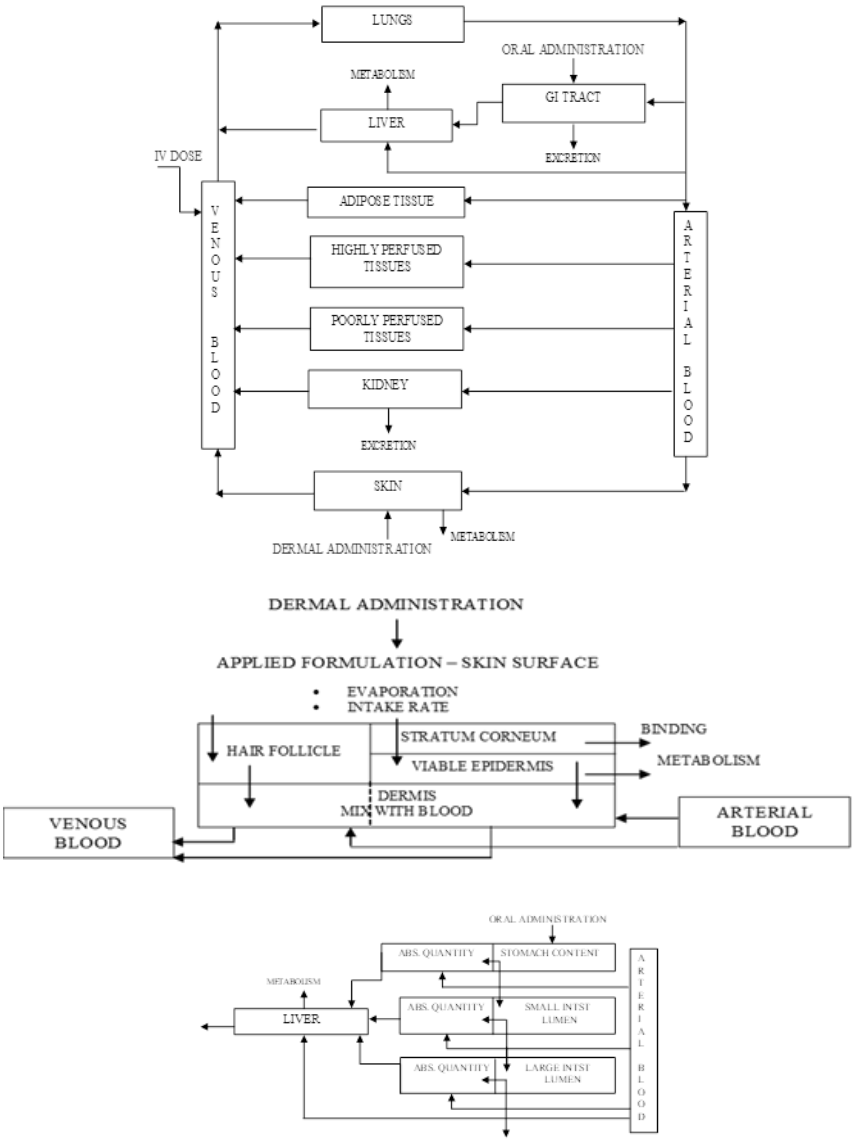

Fig. 2 Overall PBK model structures.

We illustrate the integrated use of different modelling approaches to simulate the *in vivo* kinetics of dermally applied caffeine. At the heart of this are a series of PBK models that were developed here or earlier: an oral rat

model and a dermal human model for which some elimination parameters were calibrated using oral human volunteer data and the dermal absorption by using dermal human volunteer data.

The PBK modelling approach was based on the following assumptions:

a) In the human models, skin and GI tract are represented by sub-compartments, Fig. 2. The sub-compartments account for the complexity of the absorption process (especially the time-lag in absorption). In the rat PBK model the GI tract is represented by a single compartment and a first order rate absorption is assumed.
b) In the human PBK model for oral absorption, the GI tract is represented by 6 sub-compartments (Fig. 2). In modelling absorption along the GI tract following gavage administration dissolution from matrix, stomach emptying rate and a first order rate of absorption from stomach, small and large intestine were taken into account.
c) In the rat PBK model for oral absorption, the GI tract is represented by a single compartment with first order rate of absorption following administration via food or water for caffeine (light meal followed directly by intake of a little water in which the caffeine was dissolved which means that exposure of the stomach is actually represented as food exposure). The value of this absorption rate and of metabolic parameters (liver metabolism) were obtained by fitting to oral rat experimental data for caffeine (Mohiuddin et al., 2009).
d) For PBK modelling of human dermal exposure, 4 compartments were used for dermal exposure (surface compartment for the product formulation and 3 skin sub-compartments: *stratum corneum*, viable epidermis and dermis perfused by blood), with the addition of one extra skin sub-compartment representing hair follicles (see Fig. 2). This model was selected because it gave the best goodness of fit (Gajewska et al., 2014).
e) Unidirectional diffusion describes the one-way transport in fine skin (skin without hair follicles) and hair follicles according to Fick's second law with specified initial and boundary conditions. The diffusion coefficients are different for the *stratum corneum*, viable epidermis and hair follicles and assumed constant throughout the skin absorption process. It is assumed that the test compound is applied onto the skin surface in a pure solvent (vehicle) to account for a simple formulation (i.e. in ethanol, acetone). No mixture effects are considered and the vehicle is assumed to disappear from the skin surface (in model constructed as separate compartment) only due to possible evaporation.
f) Metabolism is assumed to occur only in the liver.
g) The liver metabolism was assumed to follow Michaelis–Menten kinetics. The Vmax and Km used in the present work are reported in Gajewska et al., 2014.
h) Excretion via urine is described by a first order rate constant.
i) Tissues are assumed to be homogenised compartments with respect to the concentration of a chemical (instantaneous distribution of chemical or metabolite once it is delivered by the arterial blood). Transport between blood and tissues is assumed to be flow-limited (assuming that transport barriers between free molecules of chemical in blood and tissue are negligible) and equilibrium between free and bound fractions in blood and tissue is instantaneous. We used the QSAR-based Schmitt approach to calculate a partition between the blood and the organs of interest (Schmitt, 2008). The model calculates steady-state tissue:plasma partition coefficients based on the composition of the tissues in terms of water, neutral lipids, neutral and acidic phospholipids and proteins using the lipophilicity, the binding to phospholipid membranes, the pKa and the unbound fraction in blood plasma as compound specific parameters. For caffeine, calculations were done for pKa 10.4, LogPoct = −0.07 (octanol-water partition coefficient) and fu = 0.65 (fraction bound to proteins).
j) Inter-individual differences in metabolism and excretion are not explicitly considered (only deterministic modelling). To partially account for such variations, the metabolic rates are corrected by the subject's body weight.

Step 3. Model parameterisation (parameter estimation and analysis)

Anatomical/physiological parameters for rats and humans (reference woman and reference man) were taken from literature (Brown et al., 1997) and listed in the table A1. All physiological parameters for a reference man, woman and rat that are independent of the chemical and constitute a constant part of the model equations (see step 3). The ADME parameters for oral and dermal absorption of caffeine are given in Table A2. For the oral human model, the most sensitive parameters (GIT dissolution rates, first order uptake rate constants and metabolism parameters for liver) were optimized using measured human data. Liver metabolism parameters were taken from the literature and were optimized with respect to *in vivo* blood concentrations using human data for the main metabolites (Gajewska et al., 2015).

As reported in Gajewska et al. (2015) *in vivo* plasma concentrations of caffeine following oral absorption were taken from: (i) Lelo et al. (1986) where a non-smoking male volunteer ingested only once 270 mg of caffeine in a gelatin capsule followed by 150 mL of water; (ii) Csajka et al. (2005) where caffeine was given orally in a gelatin capsule (200 mg of caffeine sulphate) to 16 subjects and in a commercial dietary supplement (a mixture containing 200 mg caffeine and 20 mg ephedrine alkaloids) to 8 subjects. For model validation, plasma concentrations from the oral study by Newton et al. (1981) were selected, in which a gelatin capsule containing 300 mg of caffeine was administered to one male subject. Plasma caffeine levels after dermal absorption were taken from Otberg et al. (2008). In this experiment caffeine in an ethanol/propylene glycol vehicle was administered to 6 male volunteers by applying the liquid onto a chest area of 25 cm^2 for 24 h. In contrast to other dermal absorption studies, the additional impact of hair follicles in the overall absorption process was considered.

The equations of the QSARs applied for assessing dermal bioavailability are given in Gajewska et al. (2014). A review of *in vitro* and QSAR methods for predicting dermal absorption is given in Dumont et al. (2015). In order to explore models for predicting liver and skin metabolism the OECD QSAR Toolbox was applied. For caffeine, five metabolites were predicted by a QSAR approach for liver metabolism and one for skin metabolism. However, in case of skin metabolism, neither *in vitro* nor *in vivo* data were found with respect to the relevance, quantity and/or the metabolic rate constants (V_{max}, K_m). Therefore, the formation of these metabolites was not included in the PBK model.

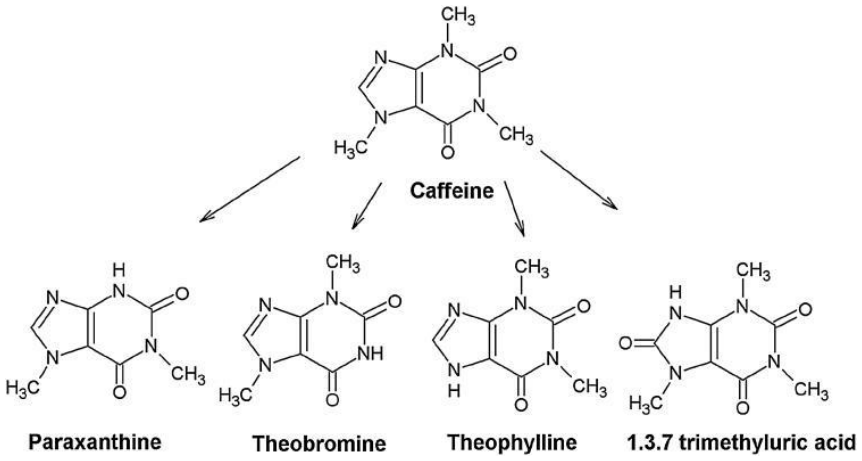

Figure 3. Caffeine MoA: metabolites formation

Step 4 – Computer implementation (solving the equations)

The mathematical equations were programmed in R language by combining functionalities of the following R packages available from "The Comprehensive R Archive Network" website (http://cran.r-project.org): deSolve, ReacTran, PK, FME, rgenoud and AICcmodavg. Ordinary differential equations (ODEs) were solved by the method *lsoda* available in the deSolve package. The method of lines was used to solve partial differential equations (PDEs). Further details of the mathematical equations are given in Appendix A1 in Supplementary material.

Mathematical equations for the PBK models (Gajewska et al., 2014; 2015)

- Adipose tissue and highly- and poorly-perfused tissues

$$\frac{dA_{org}}{dt} = f_{org} \cdot \left(C_{art} - \frac{C_{org}}{PC_{org}} \right), \quad A_{org}(t=0) = 0, \quad C_{art} = \frac{C_{art}}{V_{art}} \quad C_{org} = \frac{A_{org}}{V_{org}} \tag{A1.1}$$

where: org = organ name (adp, hpt, ppt)

- Metabolism is assumed to occur mainly in the liver

$$\frac{dA_{liv}}{dt} = Fl_{GIT} + FORM_{liv} + f_{l_{iv}} \cdot \left(C_{art} - \frac{C_{liv}}{PC_{liv}} \right) - MET_{liv}, \quad A_{liv}(t=0) = 0, \quad C_{liv} = \frac{A_{liv}}{V_{liv}} \tag{A1.2}$$

Where, for a parent compound:

$$Human: Fl_{GIT} = fra \cdot f_{git} \cdot \frac{C_{stm}}{PC_{git}} + frb \cdot f_{git} \cdot \frac{C_{SI}}{PC_{git}} + frc \cdot f_{git} \cdot \frac{C_{LI}}{PC_{git}}$$

$$Rat: Fl_{GIT} = ka_{GI,rat} \cdot \frac{C_{GI,rat}}{PC_{GI,rat}}$$

$FORM_{liv} = 0$ (rate of formation of metabolites)

In most cases, metabolism was assumed to follow Michaelis–Menten kinetics (A1.3) or was described by the first order reaction (A1.4). The liver metabolic parameter values as calibrated and optimised using the oral human volunteer data were taken unchanged to the human dermal model.

$$\frac{V_{max} \cdot \frac{C_{liv}}{PC_{liv}}}{K_m + \frac{C_{liv}}{PC_{liv}}} \tag{A1.3}$$

$$K_{\text{met}} \cdot \frac{C_{liv}}{PC_{liv}} \tag{A1.4}$$

where:

C_{liv} is the liver concentration and PC_{liv} is the liver-to-blood partition coefficient of a substance undergoing metabolism.

$$\frac{dA_{kid}}{dt} = f_{kid} \cdot \left(C_{art} - \frac{C_{kid}}{PC_{kid}} \right) - CLR \cdot \frac{C_{kid}}{PC_{kid}} \tag{A1.5}$$

Venous blood mass balance is as follows:

$$\frac{dA_{ven}}{dt} = f_{liv} \cdot \frac{C_{liv}}{PC_{liv}} + f_{ppt} \cdot \frac{C_{ppt}}{PC_{ppt}} + f_{hpt} \cdot \frac{C_{hpt}}{PC_{hpt}} + f_{adp} \cdot \frac{C_{adp}}{PC_{adp}} + f_{kid} \cdot \frac{C_{kid}}{PC_{kid}} + Fl_{skn} - f_{crd} \cdot C_{ven}, \quad A_{ven}(t=0) = 0, \quad C_{ven} = \frac{A_{ven}}{V_{ven}} \tag{A1.6}$$

where, for dermal absorption only: $Fl_{skn} = \frac{3}{4} \cdot f_{skn} \cdot \frac{C_{skn}}{PC_{skn}} + \frac{1}{4} \cdot f_{skn} \cdot \frac{C_{sknhf}}{PC_{skn}}$ otherwise $Fl_{skn} = 0$

We assume that plasma accounts for 55% of blood volume.

Plasma quantification: $$C_{ven,PL} = \frac{A_{ven} / (0.55 \cdot V_{ven})}{RBP} \tag{A1.7}$$

Arterial blood mass balance:

$$\frac{dA_{\ln g}}{dt} = f_{\ln g} \cdot \left(C_{ven} - \frac{C_{\ln g}}{PC_{\ln g}} \right); \quad A_{\ln g}(t=0) = 0; \quad C_{\ln g} = \frac{A_{\ln g}}{V_{\ln g}} \tag{A1.8}$$

$$\frac{dA_{art}}{dt} = f_{crd} \cdot \left(\frac{C_{\ln g}}{PC_{\ln g}} - C_{art} \right); \quad A_{art}(t=0) = 0 \tag{A1.9}$$

Oral Rat absorption

A single compartment representing the GI tract with first order rate of absorption:

$$\frac{dA_{GI,rat}}{dt} = -ka_{GI,rat} \cdot \frac{C_{GI,rat}}{PC_{GI,rat}} \tag{A1.10}$$

Human GI tract model consists of sub-compartments:

Stomach content: $$\frac{dA_{stm,cont}}{dt} = D_{rt} - ka_{stm} \cdot C_{stm,cont} - kGIT \cdot A_{stm,cont} \quad \text{(A1.11)}$$

with: $$C_{stm,cont} = \frac{A_{stm,cont}}{V_{stm}}, \qquad kGIT = \frac{k_{\max}}{(1 + k_{\min} \cdot C_{stm})}$$

and:

administration via gavage: $$D_{rt} = 0 \text{ and } A_{stm,cont}(t=0) = Dose$$

administration by a coated tablet: $$D_{rt} = Diss \cdot \frac{dA_{stm,cont,diss}}{dt} \text{ and } A_{stm,cont,diss}(t=0) = dose,\ A_{stm,cont}(t=0) = 0$$

Stomach tissue:

$$\frac{dA_{stm}}{dt} = ka_{stm} \cdot C_{stm,cont} + fra \cdot f_{git} \cdot \left(C_{art} - \frac{C_{stm}}{PC_{git}} \right), \quad A_{stm}(t=0) = 0, \quad C_{art} = \frac{A_{art}}{V_{art}}, \quad C_{stm} = \frac{A_{stm}}{V_{stm}} \quad \text{(A1.12)}$$

Small intestine lumen and absorbed quantity:

$$\frac{dA_{SI,lumen}}{dt} = kGIT \cdot A_{stm,cont} - (ka_{SI} + flow_{LI}) \cdot C_{SI,lumen}, \qquad A_{SI,lument}(t=0) = 0, \qquad C_{SI,lumen} = \frac{A_{SI,lumen}}{\left(\frac{3}{4} \cdot V_{\text{int}}\right)} \quad \text{(A1.13)}$$

$$\frac{dA_{SI}}{dt} = ka_{SI} \cdot C_{SI,lumen} + frb \cdot f_{git} \cdot \left(C_{art} - \frac{C_{SI,}}{PC_{git}} \right), \qquad A_{SI}(t=0) = 0, \qquad C_{SI} = \frac{A_{SI}}{\left(\frac{3}{4} \cdot V_{\text{int}}\right)} \quad \text{(A1.14)}$$

Large intestine lumen and absorbed quantity:

$$\frac{dA_{LI,lumen}}{dt} = flow_{LI} \cdot C_{SI,lumen} - \left(kel_{LI} + ka_{LI}\right) \cdot C_{LI,lumen}, \qquad A_{LI,lumen}(t=0) = 0, \qquad C_{LI,lumen} = \frac{A_{LI,lumen}}{\left(\frac{1}{4} \cdot V_{\text{int}}\right)} \quad \text{(A1.15)}$$

$$\frac{dA_{LI}}{dt} = ka_{LI} \cdot C_{LI,lumen} + frc \cdot f_{git} \cdot \left(C_{art} - \frac{C_{LI}}{PC_{git}} \right), \qquad A_{LI}(t=0) = 0, \qquad C_{LI} = \frac{A_{LI}}{\left(\frac{1}{4} \cdot V_{\text{int}}\right)} \quad \text{(A1.16)}$$

Skin surface:

$$or(t < t_{appl})\ AbsRate = -(ka_{form} \cdot C_{form} + ka_{hf} \cdot C_{form}) \text{ and } for(t > t_{appl})\ AbsRate = 0 \quad \text{(A1.17)}$$

Where: t_{appl} is the application time of a formulation on the skin.

Evaporation of a vehicle (EvapRate) is calculated for volatile substances according to Tibaldi *et al.,* (Tibaldi, ten Berge, & Drolet, 2011):

$$EvapRate = \frac{-k_{evp}}{TL} \tag{A1.18}$$

For a vehicle (solvent) this evaporation is quantified in terms of decrease of an applied solution volume in time rather than mass of the solvent:

$$\frac{dV_{appliedForm}}{dt} = -\frac{k_{evp} \cdot Area}{1000 \cdot \sigma_{form}} \qquad V_{appliedForm}(t=0) = V_{0,appliedForm} \tag{A1.19}$$

where: $k_{evp} = \frac{\beta \cdot MW \cdot V_p}{R \cdot T \cdot 10}\left[\frac{mg}{h \cdot cm^2}\right] \qquad \beta = \frac{0.0111 \cdot v_{air}^{0.96} \cdot D_g^{0.19}}{\upsilon^{0.15} \cdot X^{0.04}}$

where β is the mass transfer coefficient in vapour phase (m h^{-1}), *MW* the molecular weight, V_p the vapour pressure of the liquid at skin temperature (Pa), *R* the gas constant in J $mol^{-1}K^{-1}$, *T* the skin temperature (assumed to be 303K which equals 29.85°C), V_{air} the velocity of air (at workplaces it ranges from 0.3-0.6 m s^{-1}), D_g the diffusivity of the liquid in gas phase (range: 0.03 to 0.06 m^2h^{-1}), ϑ the kinematic viscosity of air (literature value of 0.054 m^2 h^{-1}), *X* the length of evaporation area in the direction of air stream, *TL* a thickness of applied substance layer (cm), *Area* the application area (cm^2) and δ_{form} the density of solvent (g cm^{-3}).

<u>*Stratum corneum (SC):*</u>

Passive diffusion is modelled according to Fick's second law of unidimensional diffusion with initial and boundary conditions (t_{appl} is a time of experiment duration, after which the remaining formulation is wiped off from skin surface). The diffusion coefficient is assumed to be constant throughout the process:

$$\frac{dC_{SC,i}}{dt} \approx -\frac{q_{SC,i+1} - 2 \cdot q_{SC,i} + q_{SC,i-1}}{\left(\frac{Lsc}{N}\right)}; i = 1:N \qquad C_{SC,i} = \frac{A_{SC,i}}{V_{SCi}} \tag{A1.20}$$

where: $q_{SC.,i} = -Dsc_i \cdot \frac{C_{SC,i+1} - 2 \cdot C_{SC,i} + C_{SC.,i-1}}{\left(\frac{Lsc}{N}\right)}; i = 1:N$

Initial and boundary conditions:

$$C_{SC}(t=0)|_{0\le x\le L_{SC}}=0$$
$$\frac{dC_{SC}}{dt}(t>0)|_{x=0}=ka_{form}\cdot C_{form}$$
$$D_{SC}\cdot\frac{dC_{SC}}{dx}(t>t_{appl})|_{x=0}=0$$
$$C_{SC}(t>0)|_{x=0}=PC_{SC}\cdot C_{form}$$
$$C_{SC}(t>0)|_{x=L_{SC}}=PC_{SCVE}\cdot C_{VE}$$

Viable epidermis (VE):

The reaction-diffusion partial differential equations for viable epidermis are solved in the same manner, by means of the methods of lines approach:

$$\frac{dC_{VE,j}}{dt}\approx-\frac{q_{VE,j+1}-2\cdot q_{VE,j}+q_{VE,j-1}}{\left(\frac{Lve}{M}\right)}-\frac{BioC_{VE,j}}{V_{VE,j}};j=1:M\qquad C_{VE,j}=\frac{A_{VE,,j}}{V_{VE\,j}}\tag{A1.21}$$

$$q_{VE,j}=-D_{VE,j}\cdot\frac{C_{VE,j+1}-2\cdot C_{VE,j}+C_{VE,j-1}}{\left(\frac{L_{VE}}{M}\right)};j=1:M\quad\text{and}\quad BioC_{VE,j}=\frac{V\max_{m,j}\cdot C_{VE,j}}{Km_m+C_{VE,j}}$$

Where:

Initial and boundary conditions:

$$C_{VE}(t=0)|_{0\le y\le L_{VE}}=0$$
$$C_{VE}(t>0)|_{y=0}=\frac{C_{SC,i=N}}{PC_{SCVE}}$$
$$D_{SC}\frac{dC_{SC}}{dx}|_{x=L_{SC}}=D_{VE}\cdot\frac{dC_{VE}}{dy}|_{y=0}$$
$$C_{VE}(t>0)|_{y=L_{VE}}=PC_{skn}\cdot C_{skn}$$

If skin metabolism occurs, its rate is assumed to follow first order kinetics (until more data become available). The model simulations were run for N=M=10 layers.

Dermis and mix with blood:

$$\frac{dA_{skn}}{dt}=\frac{3}{4}\cdot f_{skn}\cdot\left(C_{art}-\frac{C_{skn}}{PC_{skn}}\right)+q_{VE,j=M}\cdot\frac{100-nf}{100}\cdot Area\qquad A_{skn}(t=0)=0\qquad C_{skn}=\frac{A_{skn}}{10^{-3}\cdot\frac{2}{3}\cdot Vde}\tag{A1.22}$$

Hair follicles compartment (Bookout Jr., Quinn, & McDougal, 1997)*:*

$$\frac{dC_{hf,i}}{dt}\approx-\frac{q_{hf,i+1}-2\cdot q_{hf,i}+q_{hf,i-1}}{\left(\frac{Lhf}{K}\right)};i=1:K\qquad L_{hf}=\frac{388}{560}\cdot L\tag{A1.23}$$

$$q_{hf.,i} = -D_{hf_i} \cdot \frac{C_{hf.,i+1} - 2 \cdot C_{hf.,i} + C_{hf.,i-1}}{\left(\frac{L_{hf}}{K}\right)}; i = 1:K$$

The initial and boundary conditions:

$$C_{hf}(t=0)|_{0 \le x \le L_{hf}} = 0$$

$$\frac{dC_{hf}}{dt}(t>0)|_{x=0} = ka_{hf} \cdot C_{form}$$

$$D_{hf} \cdot \frac{dC_{hf}}{dx}(t > t_{appl})|_{x=0} = 0$$

$$C_{hf}(t>0)|_{x=0} = PC_{hf,} \cdot C_{form}$$

$$C_{hf}(t>0)|_{x=L_{hf}} = PC_{Skn} \cdot C_{sknhf}$$

Hair follicles: mix with blood

$$\frac{dA_{sknhf}}{dt} = \frac{1}{4} \cdot f_{skn} \cdot \left(C_{art} - \frac{C_{sknhf}}{PC_{skn}}\right) + q_{hf,i=K} \cdot \frac{nf}{100} \cdot Area \qquad A_{sknhf}(t=0) = 0 \qquad C_{sknhf} = \frac{A_{sknhf}}{10^{-3} \cdot \frac{1}{3} \cdot Vde} \tag{A1.24}$$

List of symbols

Symbol	Parameter [unit]
A_{org}	amount of a chemical in organ/tissue [mg]
Area	application area on skin [cm^2]
CLR	renal clearance rate [L/h]
C_{org}	concentration of a chemical in organ/tissue [mg/L]
D_{HF}	diffusion coefficient in coefficient in hair follicles [cm^2/h]
Diss	dissolution from a coated matrix [L/h]
D_{SC}	diffusion coefficient *in stratum corneum* [cm^2/h]
Dt	drinking rate [L/h]
D_{VE}	diffusion coefficient in viable epidermis [cm^2/h]
f_{crd}	cardiac output [L/h]
$flow_{LI}$	flow rate from small intestine into large intestine [L/h]
f_{org}	regional blood flow rates [L/h]

Fl_{GIT}	Amount from the GI tract [mg]
Flskn	Amount from the skin [mg]
ka_{form}	intake rate of chemical from formulation by stratum corneum [mL/h]
ka_{HF}	intake rate of a chemical from formulation by hair follicles [mL/h]
ka_{LI}	absorption rate from large intestine lumen [L/h]
ka_{SI}	absorption rate from small intestine lumen [L/h]
ka_{stm}	absorption rate into stomach tissue [L/h]
$ka_{GI,rat}$	absorption rate into GI tract for rat [L/h]
kel_{LI}	elimination rate in large intestine lumen [L/h]
K_m	chemical concentration at which the reaction rate is half of the maximal [mg/L]
K_{met}	first order rate of formation of metabolites [L/h]
K_{min}, K_{max}	kinetic constants of stomach emptying rate of a chemical to small intestine [L/h]
L_{sc}	thickness of *stratum corneum* [cm]
L_{ve}	thickness of viable epidermis [cm]
$PC_{bloodair}$	blood/air partition coefficient
PC_{HF}	partition coefficient hair follicle /solvent
PC_{org}	tissue-to- blood partition coefficients
PC_{SC}	partition coefficient *stratum corneum*/ solvent
PC_{SCVE}	partition coefficient *stratum corneum*/ viable epidermis
RBP	Blood-to-plasma concentration ratio
Rem_{bld}	bladder emptying rate [L/h]
$Rform_{Creat}$	formation rate of creatinine[mg/h]
V_{max}	the maximum rate metabolic rate at maximum (saturating) concentration of a chemical [mg/h]
V_{org}	volume of organ/tissue

Step 5 – Model Performance

Parameters were analysed using the sensitivity analysis as reported in Gajewska et al. (2014). Briefly, the sensitivity analysis and parameter identifiability were performed to identify the most important and sensitive parameters with respect to the blood/plasma AUC for caffeine according to Soetaert and Petzoldt (Soetaert and Petzoldt, 2010) prior to their optimization. In local sensitivity analysis Eq. (1), all parameters were evaluated individually in a very small region close to their nominal value. A parameter value divided by the average of simulated outputs was used as a scaling factor (SF).

$$x=f(x,u,\phi)y=g(x,\phi)Sij=(\phi j0SF)\partial yi\partial\phi j|\phi=\phi 0 \quad (1)$$

$$L1=\sum||Sij||NL2=\sqrt{\sum}S2ijN \quad (2)$$

$$\gamma=1\sqrt{}\min(EV)[\hat{}sT\cdot\hat{}s] \quad (3)$$

where y is vector of function outputs for a specific variable; x is vector of state variables; θ is vector of parameters (θ 0parameter estimate); u is vector of inputs; N is number of time points;ˆs

is the columns of the sensitivity matrix that correspond to the parameters included in the set; EV is estimation of the eigenvalues.

The following kinetic and compound-specific parameters were analyzed: GItract absorption rates (D_{iss} (or D_t), k_{astm}, k_{aSI}, k_{aLI}, k_{elLI}, k_{max}, k_{min}), liver metabolic rates (V_{max}, kK_m, K_{met}), skin absorption parameters (D_{sc}, D_{ve}, D_{hf}, k_{aform}, k_{ahf}, PC_{sc},PC_{scve}, PC_{hf}), blood-to-plasma ratio and tissue-to-blood partition coefficients: PC_{liv}, PC_{adp}, PC_{ppt}, PC_{hpt}, PC_{kid}, PC_{lng}, PC_{git}, PC_{skn}. The higher the absolute sensitivity value, the more important is the parameter. These sensitivity functions are collapsed into summary values (L1 and L2 are used as selection criteria) (Eq. (2)). Based on the sensitivity functions of blood AUC to selected parameters, the identifiability of a set of parameters to be fine-tuned by calibration is then calculated. As a rule of thumb, a collinearity value (γ) less than about 20 means "identifiable" (in general, when the collinearity index exceeds 20, the linear dependence is assumed to be critical (Eq. (3)) (Brun et al., 2001). The collinearity is a measure of approximate linear dependence between sets of parameters. The higher its value, the more the parameters are related. In this context, "related" means that several parameter combinations may produce similar values of the output variables.

Monte Carlo simulations were used to quantify the impact of variability and uncertainty in parameter distributions separately by drawing parameter values according to a predefined distribution (normally distributed random samples), running the model with each of these parameter combinations, and calculating the values of the selected output variables at each output interval. The parameters were optimized according to the Levenberg-Marquardt algorithm for nonlinear data fitting (Moré, 1978).

With an oral exposure to caffeine, the tissue-to-blood partition coefficients show comparable sensitivity to kinetic parameters in terms of blood/plasma AUC; however, lower sensitivity is observed in the case of dermal absorption. The most sensitive kinetic parameters are caffeine metabolic rate to paraxanthine (V_{max}), skin absorption rates (D_{sc}, D_{ve}, D_{hf}) and blood-to-plasma ratio. The most sensitive partition coefficients are: PC_{adp}, PC_{ppt}, PC_{kid} (oral model) and PC_{lng}, PC_{adp}, PC_{ppt} (dermal model).

Simulation graphs are available in the paper by Bessems et al., 2017.

Step 6 – Model Documentation

Bessems et al., 2017

E. Identification of uncertainties

model structure

- The human models, skin and GI tract are represented by sub-compartments, fig 2. The sub-compartments account for the complexity of the absorption process (especially the time-lag in absorption). In the rat PBK model the GI tract is represented by a single compartment and a 1st order rate absorption is assumed.
- Metabolism is assumed to occur only in the liver.
- First order oral absorption, first order oral absorption has been stated to be applicable to many pharmaceuticals. However, for non-pharmaceuticals, this is uncertain. Also, the value for the first order absorption rate constant used may change for significantly different exposure conditions. Predicted AUC as well as C_{max}values may deviate significantly from the real AUC and C_{max}(rat, human). The potential risk is significant over- or underestimation of actual risk

- No human first pass metabolism in skin. First pass metabolism reduces the internal exposure to the parent chemical. Internal exposure to the parent chemical is overestimated (either as AUC or as Cmax). No consequence in comparison to default approach (just using total external dose). Larger risks predicted compared to when first pass metabolism in skin would have been taken into account.

input parameters

- The model calculates steady-state tissue:plasma partition coefficients based on the composition of the tissues in terms of water, neutral lipids, neutral and acidic phospholipids and proteins using the lipophilicity, the binding to phospholipid membranes, the pKa and the unbound fraction in blood plasma as compound specific parameters. For caffeine, calculations were done for pKa 10.4, LogPoct = −0.07 (octanol-water partition coefficient) and fu = 0.65 (fraction bound to proteins).
- No genetic polymorphism in the human population. The values used for Vmax and Km in the present work are not representative for the whole human population (it is known that there is genetic polymorphism).

model output

- No genetic polymorphism in the human population
- Predicted AUC and Vmax are not valid for the whole human population. Risks may be over- or under predicted for part of the human population.

other uncertainties (e.g. model developed for different substance and/or purpose)

F. Model implementation details

- software (version no) Not reported
- availability of code Available upon request, SEURAT 1 /COSMOS output
- software verification / qualification Not applicable

G. Peer engagement (input/review)

Not peer reviewed.

H. Parameter tables

Table A1. Anatomical and physiological parameters for a reference woman, a reference man and rat (Brown et al., 1997)

Parameter	Reference woman	Reference man	Rat
Average body weight [kg]	65	75	0.265
Organ weights fractions (fractions of body weight)			
Liver	0.026	0.026	0.0253
Adipose tissue	0.278	0.155	0.07
Lungs	0.0105	0.012	0.005

Kidney	0.0044	0.0044	0.0073
GI tract total	0.0265 *	0.025 *	0.046
Stomach	0.00337	0.00318	
Small intestine	0.0146	0.0138	
Large intestine	0.0085	0.0080	
Poorly perfused tissues + skin	0.436	0.525	0.667
Highly perfused tissues	0.153	0.181	0.1254
Blood total	0.065	0.072	0.054
Venous blood	0.04875	0.054	0.018
Thickness of skin [cm]			
Whole skin	0.204	0.2906	0.17
Viable epidermis	0.0032	0.0047	0.001
Stratum corneum	0.0018	0.0017	0.002
Dermis	?	?	?
Organ and tissue blood flow rates [fraction of cardiac output [L/h]			
Cardiac output [L/h]	$15 \cdot BW^{0.74}$		5.208
Liver	0.25	0.24	0.009
Adipose tissue	0.055	0.04	0.07
Skin	0.05	0.05	0.058
Highly perfused tissues	0.155	0.155	0.222
Poorly perfused tissues	0.135	0.16	0.4
Kidney	0.19	0.2	0.14
GI tract	0.14	0.13	0.08
Lungs	0.025	0.025	0.021

* Sum of stomach, small intestine and large intestine

Table A2. Human and Rat oral physiological parameters and ADME parameters for caffeine[1]

Parameter	Value
Physiological parameters oral	
Stomach emptying maximum rate k_{max} [L/h]	8.16 (Loizou & Spendiff, 2004)
Stomach emptying rate k_{min} [L/h]	0.005 (Loizou & Spendiff, 2004)
Release from formulation/matrix/capsule	
Dissolution from matrix Diss [L/h]	3.2
Absorption oral	
Stomach 1st order absorption rate constant ka_{stm} [L/h]	0.2
Small intestine 1st order absorption rate constant ka_{si} [L/h]	1.5
Large intestine elimination kel_{li} [L/h]	0.1
Absorption dermal	
Diffusion coefficient in stratum corneum D_{sc} [cm^2/h]	1.4e-07 (Hansen et al., 2008)
Diffusion coefficient in viable epidermis D_{ve} [cm^2/h]	1.5e-05 [2]
Diffusion coefficient in hair follicles D_{hf} [cm^2/h]	1.243e-05
Formulation intake rate from stratum corneum ka_{form} [mL/h]	0.2
Formulation intake rate from hair follicles ka_{hf} [mL/h]	0.153
Partition coefficient stratum corneum/vehicle PC_{sc}	2.5 (Hansen et al., 2008)
Partition coefficient stratum corneum/viable epidermis PC_{scve}	0.6 [2]
Partition coefficient hair follicles/vehicle PC_{hf}	1 [3]
% of hair follicles in skin (nf)	20
Blood/plasma ratio and tissue to blood partition coefficients (Schmitt, 2008)	
Blood-to-plasma ratio RBP	0.28-0.35 (Newton et al., 1981)
Liver: PC_{liv}	4.25

Poorly-perfused tissues: PC_{ppt}	0.995
Highly-perfused tissues:PC_{hpt}	1
Skin: PC_{skn}	1
Lungs: PC_{lng}	1.23
Kidney: PC_{kid}	3.76
GI tract: PC_{git}	1.49
Adipose tissue: PC_{adp}	0.68
Michaelis-Menten parameters	
caffeine to paraxanthine	V_{max} = 0.351[4]; K_m= 1
caffeine to theobromine	V_{max} = 0.0432; K_m=1 (Lelo et al., 1986; Zandvliet et al., 2005)
caffeine to theophylline	V_{max} = 0.0072; K_m=1 (Lelo et al., 1986; Zandvliet et al., 2005)
caffeine to trimethyluric acid	K_{met}=0.001 (Lelo et al., 1986; Zandvliet et al., 2005)

[1] Values without footnote or reference were fitted to experimental data; [2] Estimated by QSPRs; [3] PC_{hf} was set at 1 as no QSARs were found to predict it. Optimising it to a calibration set did not make sense as the diffusion coefficient had to be optimised as well and the two are strongly correlated. As the model is more sensitive to diffusion coefficient it was decided to optimise only that value in the usual range of values of diffusion coefficient (10^{-5}) and to set PC_{hf} for caffeine at 1, being a reasonable value between the usual boundaries of approx. 0.5 and 8 seen so far with this sort of chemicals; [4] Predicted by ADMET Predictor (https://www.simulations-plus.com/)

I. References and background information

- publications

Bookout Jr., R.L. Quinn, D.W. McDougal J.N. (1997) Parallel dermal subcompartments for modeling chemical absorption. SAR QSAR Environ. Res., 7, pp. 259–279.

Brown, R.P., Delp, M.D Brown, R.P., Delp, M.D., Lindstedt, S.L., Rhomberg, L.R., Beliles, R.P., 1997. Physiological parameter values for physiologically based pharmacokinetic models. Toxicol. Ind. Health 13, 407–484.., Lindstedt, S.L., Rhomberg, L.R., Beliles, R.P., 1997. Physiological parameter values for physiologically based pharmacokinetic models. Toxicol. Ind. Health 13, 407–484.

Gajewska, M., Worth, A., Urani, C., Briesen, H., & Schramm, K. (2014). Application of physiologically-based toxicokinetic modelling in oral-to-dermal extrapolation of threshold doses of cosmetic ingredients. Toxicol Lett., 227(3).

Gajewska, M., Paini A., Sala Benito J, Burton J, Worth, A., Urani, C., Briesen, H., & Schramm, K. (2015). In vitro to in vivo correlation of the skin penetration, liver clearance and hepatotoxicity of caffeine. Food and Chemical Toxicology, 75, 39–49.

Hansen, S., Henning, A., Naegel, A., Heisig, M., Wittum, G., Neumann, D., … Schaefer, U. F. (2008). In-silico model of skin penetration based on experimentally determined input parameters. Part I: Experimental determination of partition and diffusion coefficients. European Journal of Pharmaceutics and Biopharmaceutics, 68(2), 352–367.

Lelo, A., Birkett, D. J., Robson, R. A., & Miners, J. O. (1986). Comparative pharmacokinetics of caffeine and its primary demethylated metabolites paraxanthine, theobromine and theophylline in man. British Journal of Clinical Pharmacology, 22(2), 177–182. Retrieved from http://www.scopus.com/inward/record.url?eid=2-s2.0-0023025836&partnerID=40&md5=aff5345dfec1380a75a9781e56072faf

Loizou, G. D., & Spendiff, M. (2004). A human PBPK model for ethanol describing inhibition of gastric motility. Journal of Molecular Histology, 35(7), 687–696.

Newton, R., Broughton, L. J., Lind, M. J., Morrison, P. J., Rogers, H. J., & Bradbrook, I. D. (1981). Plasma and salivary pharmacokinetics of caffeine in man. European Journal of Clinical Pharmacology, 21(1), 45–52.

Tibaldi, R. ., ten Berge, W., & Drolet, D. (2011). IH SkinPerm Help Manual.

Zandvliet, A. S., Huitema, A. D. R., De Jonge, M. E., Den Hoed, R., Sparidans, R. W., Hendriks, V. M., … Beijnen, J. H. (2005). Population pharmacokinetics of caffeine and its metabolites theobromine, paraxanthine and theophylline after inhalation in combination with diacetylmorphine. Basic and Clinical Pharmacology and Toxicology, 96(1), 71–79. Retrieved from http://www.scopus.com/inward/record.url?eid=2-s2.0-13844310313&partnerID=40&md5=b27d1606e33e9ae71c458ac3421c660f

Part II Checklist for model evaluation

PBK Model Evaluation Checklist	Checklist assessment	Comments
Name of the PBK model (as in the reporting template)		
Model developer and contact details		
Name of person reviewing and contact details		
Date of checklist assessment		
A. Context/Implementation		
A.1. Regulatory Purpose		
1. What is the acceptable degree of confidence/uncertainty (e.g. high, medium or low) for the envisaged application (e.g. priority setting, screening, full assessment?)		
2. Is the degree of confidence/uncertainty in application of the PBK model for the envisaged purpose greater or less than that for other assessment options (e.g. reliance on PBK model and *in vitro* data vs. no experimental data)?		
A.2. Documentation		
3. Is the model documentation adequate, i.e. does it address the essential content of model reporting template, including the following:		
● Clear indication of the chemical, or chemicals, to which the model is applicable?		
● Is the model being applied for the same scientific purpose as it was developed, or has it been repurposed somehow?		
● Model assumptions?		
● Graphical representation of the proposed mode of action, if known?		
● Graphical representation of the conceptual model?		
● Supporting tabulation for parameters (names, meanings, values, mean and standard deviations, units and sources)?		
● Relevance and reliability of model parameters?		
● Uncertainty and sensitivity analysis?		
● Mathematical equations?		
● PBK model code?		
● Software algorithm to run the PBK model code?		
● Qualification of PBK software platform?		
A.3 Software Implementation and Verification		
4. Does the model code express the mathematical model?		

5. Is the model code devoid of syntactic and mathematical errors?		
6. Are the units of input and output parameters correct?		
7. Is the chemical mass balance respected at all times?		
8. Is the cardiac output equal to the sum of blood flow rates to the tissue compartments?		
9. Is the sum total of tissue volumes equal to total body volume?		
10. Is the mathematical solver a well-established algorithm?		
11. Does the mathematical solver converge on a solution without numerical error?		
12. Has the PBK modelling platform been subjected to a verification process (for a different use, for instance, in the pharmaceutical domain)?		
A.4 Peer engagement (input/review)		
13. Has the model been used previously for a regulatory purpose?		
● Is prior peer engagement in the development and review of the model sufficient to support the envisaged application?		
● Is additional review required? Peer engagement includes input/review by experts on specific aspects of model development, individual reviews of the model by experts, or collective reviews by peer review panels. Availability of the comments and tracking of revisions to the model in response to peer input contributes to increased confidence in the model for potential application.		
B. Assessment of Model Validity		
B.1 Biological Basis (Model Structure and Parameters)		
14. Is the model consistent with known biology?		
● Is the biological basis for the model structure provided?		
● Is the complexity of the model structure appropriate to address the regulatory application?		
● Are assumptions concerning the model structure and parameters clearly stated and justified?		
● Is the choice of values for physiological parameters justified?		
● Is the choice of methods used to estimate chemical-specific ADME parameters justified?		
● Saturable Kinetics		
B.2 Theoretical Basis of Model Equations		

15. Are the underlying equations based on established theories, .e.g. Michaelis-Menten kinetics, Fick's laws of diffusion?		
● In the case of PBK models for particles, does the model take into consideration the properties of particles, e.g. particle size ranges, (poor) solubility, aggregation, partitioning and diffusion/sedimentation behaviour?		
B.3. Reliability of input parameters		
16. Has the uncertainty (individual variability, experimental reproducibility and reliability) in the input parameters been characterised?		
B.4. Uncertainty and Sensitivity Analysis		
17. Has the impact of uncertainty (individual variability, experimental reproducibility and reliability) in the parameters on the chosen dose metric been estimated?		
● Local sensitivity analysis?		
● Global sensitivity analysis?		
18. Is confidence in influential input parameter estimates (i.e., based on comparison of uncertainty and sensitivity) reasonable (within expected values; similar to those of analogues) in view of the intended application?		
B.5. Goodness-of-Fit and Predictivity		
19. For PBK models for which there are sufficient *in vivo* data for the chemical of interest:		
● Suitability as analogue (chemical and biological similarity) been assessed?		
● Reliable estimation of chosen dose metric for analogue?		
● In general is the biological Variability of *in vivo* reference data (from analogue) established?		

NA = not applicable, NR not reported

Part III Overall Evaluation

Overall Conclusion on mode evaluation for the intended application